

CCD-based X-ray area detector for time-resolved diffraction experiments

Naoto Yagi,* Katsuaki Inoue and Toshihiko Oka‡

SPring-8/JASRI, Kouto, Mikazuki, Sayo, Hyogo 679-5198, Japan. E-mail: yagi@spring8.or.jp

A fast X-ray area detector for diffraction, scattering and imaging experiments at microsecond to millisecond time resolution has been developed. The key element of the detector is a fast (291 frames s^{-1}) framing camera with three CCDs. A prism forms identical images on the CCDs and the frame rate is increased three times by reading them alternately. In order to convert X-rays into visible light that is detectable with the CCDs, an X-ray image intensifier is used. The camera can also be used with a high-resolution X-ray detector. In both cases it was found to be important to use a phosphor with a short decay time to fully make use of the high-speed framing capability of the camera. Preliminary results of a fibre diffraction experiment on a skeletal muscle and coronary angiography are presented.

Keywords: CCD cameras; SPring-8; time-resolved; image intensifiers.

1. Introduction

In X-ray diffraction experiments, especially those carried out at synchrotron radiation facilities, CCD (charge-coupled device) detectors are now commonly used. In such detectors, X-rays are converted into visible light by a phosphor, and a CCD is used as a detector for the visible image. Although CCD chips are generally small, the active area can be made larger by using a tapered optical fibre between the phosphor and the CCD chip (Gruner & Ealick, 1995). An X-ray image intensifier can also be used to reduce the image size (Amemiya *et al.*, 1995).

Although readout of a CCD is faster than that of a film and an image plate, the maximum readout speed of commonly used CCD detectors is only a few frames per second at maximum. The frame rate is generally kept low in order to reduce readout noise. A higher frame rate is not required when the exposure is much longer than the readout time, which is actually the case in most diffraction experiments using synchrotron radiation. However, in the case of time-resolved experiments, higher seamless readout is required. As a CCD is often used in video cameras, a frame rate of 30 s^{-1} , with a pixel array of 640×480 , is easily achieved. However, as a wide dynamic range is not required for videos, the data are usually digitized in 8 bits. For quantitative diffraction experiments, a wider dynamic range is necessary. Currently, several CCD cameras are commercially available for such a purpose: for instance, C4880-80 (656×494 pixels, 12 bits, 29 frames s^{-1}) and C8800 (1000×1000 pixels, 12 bits, 30 frames s^{-1}) from Hamamatsu Photonics, and TF 1M60 (1024×1024 pixels, 12 bits, 60 frames s^{-1}) and 4M30 (2048×2048 pixels, 12 bits, 30 frames s^{-1}) from Dalsa. C4880-80 has been extensively used in time-resolved experiments at SPring-8 (see, for example, Horiuti *et al.*, 2003; Terasaki *et al.*, 2004).

Another area detector suitable for time-resolved experiments is a gas detector. Since a gas detector is a photon-counting detector, it has the advantage of having low noise. On the other hand, since a photon-

counting detector has to deal with each incident X-ray photon, the maximum count rate is limited by the performance of its electronics. The highest counting rate ever achieved by an area gas detector for synchrotron radiation experiments is $\sim 1.5 \times 10^7$ counts s^{-1} over the whole area (Lewis *et al.*, 2000). Although this counting rate is sufficient for most beamlines in second-generation synchrotron radiation facilities, the flux in third-generation facilities often exceeds this counting limit. Since the high flux is essential for experiments at high time resolution, an integrating detector such as a CCD-based detector, which does not have a limit in the counting rate, is advantageous in such newer facilities provided that it works at a high frame rate.

Another area detector, a photon-counting pixel array detector (Hülse *et al.*, 2004), may also suffer from the limit in the counting rate. On the other hand, an integrating-type pixel array detector (Rossi *et al.*, 1999) is potentially ideal for experiments with high time resolution, up to the nanosecond range, and high X-ray flux. However, a detector with a sufficiently large area and capacity to store hundreds of frames has not yet been realised, and would be very expensive even if one was constructed.

In this report, two X-ray detectors based on a fast CCD camera are described. The camera has three CCDs that operate alternately to increase the frame rate. It is combined with either an X-ray image intensifier or a high-resolution X-ray detector and used in time-resolved experiments. A brief description of this detector system has already appeared in the literature (Inoue *et al.*, 2004).

2. Methods

2.1. CCD camera

The CCD camera that we tested was a prototype of C7770 from Hamamatsu Photonics KK (Hamamatsu, Shizuoka, Japan), which has three CCD chips. Visible light from a lens enters a prism and the same images are formed on the three chips (Fig. 1). The CCD chip is an interline type (Sony ICX-074) with 656 (horizontal) \times 494 (vertical)

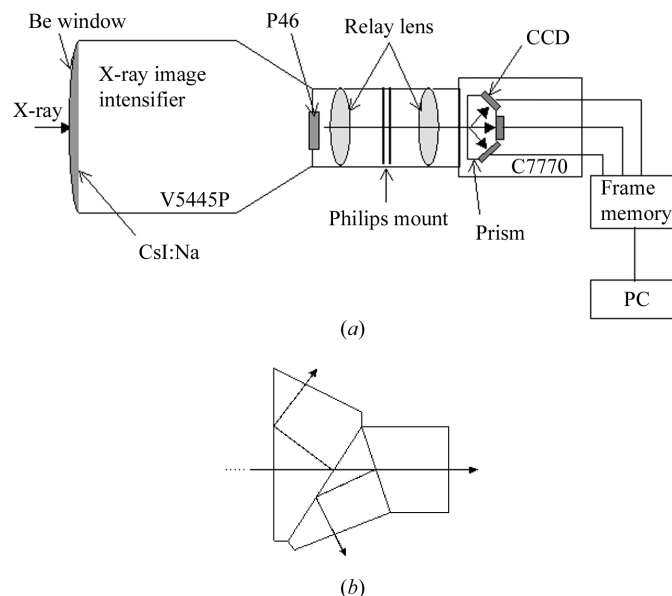


Figure 1 Schematic drawings of (a) the fast CCD camera with X-ray image intensifier, and (b) the prism used in the camera. In (a), V5445P is a beryllium-windowed X-ray image intensifier and C7770 is a fast 3-CCD camera from Hamamatsu Photonics.

‡ Present address: Department of Physics, Faculty of Science and Technology, Keio University, Japan.

pixels. Each pixel is $9.9 \mu\text{m} \times 9.9 \mu\text{m}$. The well depth is about 24000 electrons. The charges in the pixels are digitized in 10 bits, so that 1 ADU (analogue-to-digital conversion unit) corresponds to about 20 electrons. In standard operation mode (Fig. 2), each of the three chips is exposed for 3.4 ms, and then the charges are transferred in 3.6 μs to registers which are masked from light. Reading and digitizing the charges from the registers takes 10.2 ms. During this readout period, the chip is always exposed to light and accumulating charges. However, at 3.4 ms before the readout finishes, the charges are erased and the next exposure begins. When the readout finishes, the charges are transferred to the registers and the next readout begins. The same process takes place in the other two chips but with a delay of 3.4 or 6.8 ms. Thus, one of the three chips is always recording an image. By combining the readout from the three CCD chips, a seamless time-resolved recording can be made. The exposure time of each frame is 3.43 ms, providing a frame rate of 291 s^{-1} . This corresponds to a pixel rate of 94 MHz. This frame rate (not the pixel rate) can be increased by reducing the number of horizontal lines in the image. When only 140 lines are read, the exposure time can be reduced to 1.04 ms; for 72 lines and 18 lines, the exposure times are 0.53 ms and 0.163 ms, respectively ($6118 \text{ frames s}^{-1}$). In these cases, only the top area of the CCD, which is closest to the readout tap, is read. If another area is exposed to light, the charges in the area will be shifted to the top area during the readout procedure and will overlap the image recorded in the top area. Thus, it is necessary to make sure that only the area that is read out is illuminated. The frame rate can be reduced to a half or a quarter by slowing down the pixel clock.

This camera is now commercially available. However, the prototype that was used in the present study has a unique design that is not realised in the commercial product. When only the top area of the CCD chip is used to increase the frame rate, the recorded area is not the central area of the X-ray detector. This is inconvenient when the X-ray detector, which converts an X-ray image into a visible image, has distortion or low sensitivity at the periphery of its detection area. This is actually the case with an X-ray image intensifier. Thus, a mechanism was installed in the camera to move the assembly of the prism and the three CCD chips vertically. By moving the active area of the CCD to the centre of the detection area of the X-ray detector, the central part of the detector can be observed at a high frame rate.

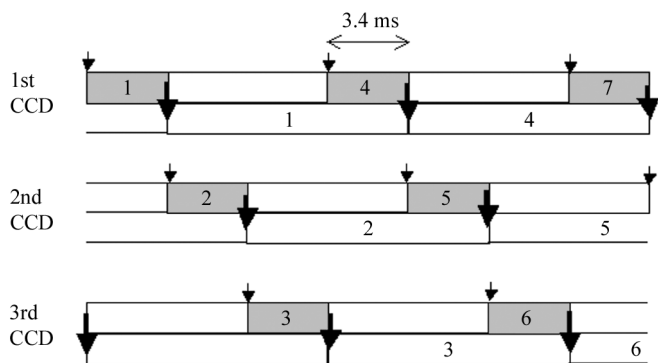


Figure 2 Timing sequence of the readout of the 3-CCD camera (C7770). The numbers indicate the frame sequence. For each CCD the upper part shows the status of the pixel that receives light, while the lower part shows that of the register for readout. The registers are masked from the light. At the small arrows, the electron charges in the pixel are erased and the exposure begins. At the large arrows, the charges are transferred to the register and then read out. The readout takes 10.2 ms. Thus, by delaying actions in the three CCDs by a multiple of 3.4 ms, it is possible to make a continuous time-resolved recording of images.

The camera is connected to a frame memory for data transfer. In the commercial product, a 2 Gbyte memory on a frame grabber (GPIO-4500, Graphin, Tokyo, Japan) is used. The prototype detector is connected to a 4 Gbyte frame memory in a separate box, which was made by Nexus Corporation (Tokyo). With 4 Gbytes, it can continuously record images for 20 s. In both cases the digital data from the three CCD chips in the camera are transferred to the memory in real time, and then later to the memory or a computer hard disk.

The camera is equipped with a square-shaped precision mount, commonly used in X-ray image intensifiers for medical use, so that it can be combined with any light-converting-type X-ray detector with the same mount. The prototype camera is equipped with a lens (F2.0, $f = 35 \text{ mm}$), which works as a tandem lens in combination with a lens in the X-ray detector.

2.2. X-ray detectors

The CCD camera was designed to be combined with an X-ray image intensifier for diffraction and scattering experiments with high time resolution. A six-inch X-ray image intensifier with a beryllium window (V5445P, Hamamatsu Photonics) has been used in small-angle scattering experiments at synchrotron radiation facilities, and its characteristics have been fully described (Amemiya *et al.*, 1995; Fujisawa *et al.*, 1999). An X-ray image intensifier has the following advantages: (i) it can reduce the image size to match the size of a CCD which is much smaller than the diffraction or scattering pattern, and (ii) it intensifies an X-ray image so that a single X-ray photon can be observed. The one used in this study has an output window of diameter 13 mm and a F1.0 lens with $f = 50 \text{ mm}$. When combined with the prototype camera by the precision mount, the two lenses work as a tandem lens and each pixel of the CCD corresponds to about $220 \mu\text{m} \times 220 \mu\text{m}$ on the beryllium window. The phosphor at the entrance window of the image intensifier is CsI:Na, with a thickness of $200 \mu\text{m}$. One modification that we made to the prototype detector was to use P46 (YAG, $\text{Y}_3\text{Al}_5\text{O}_{12}:\text{Ce}$) in the output window. This scintillator has a faster response compared with others such as P20 ($\text{ZnCdS}:\text{Ag}$) or P43 ($\text{Gd}_2\text{O}_3:\text{Tb}$), as described in the *Results* section. The X-ray image intensifier has a changeable aperture behind the lens. The area of the hole in the aperture increases by a factor of two with an increase by a factor of one in the aperture number.

X-ray image intensifiers have the drawback that a recorded image is subject to distortion (including that induced by an environmental magnetic field) and shading (Amemiya *et al.*, 1995). However, it has been shown that, when carefully used, reliable results can be obtained even in small-angle solution scattering experiments which require a wide dynamic range and linearity (Fujisawa *et al.*, 1999). In time-resolved experiments, an intensity change at a certain point (or an area) in a well studied diffraction pattern should usually be measured. Thus, distortion or shading does not cause a major problem in the interpretation of data.

Another type of X-ray detector is a high-resolution detector called a 'beam monitor' which was developed at SPring-8 (Uesugi *et al.*, 1999). This detector is made from the simple combination of a thin phosphor and a lens. It also has the same precision mount as that of C7770. The detector used in the present study (BM2) incorporated $10 \mu\text{m}$ -thick P43 and a lens (F2.8 and $f = 24 \text{ mm}$). When combined with the prototype camera, each pixel in the image was about $7 \mu\text{m} \times 7 \mu\text{m}$.

2.3. Beamline

CCD cameras are usually used in combination with an X-ray image intensifier on beamline BL40XU at SPring-8. BL40XU is a beamline specialized in delivering a high flux: radiation from a helical undulator is used without monochromatization (Inoue *et al.*, 2001). The highest flux is $\sim 1 \times 10^{15}$ counts s^{-1} , but this was reduced in the present study by using an aluminium absorber to avoid saturation of the detector. All tests were carried out with a peak X-ray energy of 12.4 keV and an energy bandpass of about 2% (full width at half-maximum) unless otherwise stated. An angiography experiment was carried out at BL20XU (Suzuki *et al.*, 2004), an undulator beamline with a Si(111) monochromator. An experiment on a rat heart, which was perfused with a Tyrode solution in a Langendorf set-up, was performed at the end-station, which is located at about 240 m from the X-ray source. The X-ray energy was 17 keV.

3. Results

3.1. C7770

3.1.1. Variation in offset, gain and position. In the prototype CCD camera, the analogue offset level of the analogue-to-digital converter was different by less than 1 ADU among the three CCDs. This can be corrected by recording more than three continuous blank frames. The difference in gain among the three CCDs was less than 6%, which can be corrected by recording a still image with all three CCDs. These offset and gain differences depend on the tuning of each camera by the manufacturer.

Although the positions of the three CCD chips were adjusted to one-third of the pixel size by the manufacturer, a small difference in the peak position was observed with the three CCDs when calculated from a weight average of pixel values around the peak (Yagi, 2003). The experimentally observed deviation was about 0.1 pixels.

To correct for these variations caused by the use of three CCDs, it is necessary to identify which CCD was used to record each image. C7770 provides a frame signal that is given only when one of the CCDs records an image, which helps to identify the CCD.

3.1.2. Noise level. The readout noise was measured in a 200 frame blank exposure for each CCD. Fluctuation in digital values was measured in ten pixels independently and averaged. The standard deviation was found to be 0.67, 0.89 and 0.92 ADU for the three CCDs, equivalent to 17 electrons on average. The difference among the three CCDs was not statistically significant.

3.2. C7770 with an X-ray image intensifier

3.2.1. Sensitivity. In this experiment a small beam (about 0.5 mm in diameter) was made by placing a lead plate with a hole within a small-angle scattering region of silica particles (mean diameter 100 nm, Seahoster KE-P10, Nippon Shokubai, Kyoto, Japan) at BL40XU. The intensity was measured by both a YAP:Ce scintillation counter (KX-101, Oken, Tokyo, Japan) and an X-ray image intensifier equipped with the C7770 or C4880-50-24A CCD camera. C4880-50-24A is a slow-scan cooled CCD camera from Hamamatsu Photonics. With the CCD cameras, the intensity within the beam was integrated after background subtraction. The flux was reduced to below 10000 counts s^{-1} to avoid saturation of the scintillation counter. The X-ray energy was 15 keV.

Assuming 100% efficiency for the scintillation counter, the conversion gain was 0.4 ADU per X-ray photon for C7770 with an aperture number 5 which passes 70% of the light from the X-ray image intensifier to the camera. For C4880-50-24A, it was 47 ADU per photon with the same aperture. 1 ADU for C7770 corresponds to about 20 electrons, while that for C4880-50-24A corresponds to about

2.8 electrons. Thus, one X-ray photon creates eight electrons in C7770 and 130 electrons in C4880-50-24A. With C4880-50-24A, it was possible to observe a single X-ray photon since its readout noise was about 10 electrons, whereas it was difficult with C7770 whose readout noise was 16 electrons (see §3.1.2). This difference is mostly accounted for by (i) the split of the beam into three beams by the prism in C7770 (three times reduction without considering the loss of light at the interfaces), (ii) the difference in the lens: C7770 was equipped with a F2.0 35 mm lens while C4880-50-24A was equipped with a F1.8 50 mm lens, (iii) different efficiencies of the CCDs: with 530 nm light, which is the peak wavelength of P46, the efficiency of C7770 (ICX-064) is 40% while that of C4880-50-24A (E2V CCD47-10, backthinned) is 80%.

The conversion ratio changed approximately in parallel with the X-ray energy below 15 keV, showing that CsI in the X-ray image intensifier (200 μm) is thick enough to absorb all photons.

3.2.2. Persistence. A solenoid-driven shutter was placed in the X-ray beam at BL40XU. Although the shutter is slow in beginning to move, it cuts the X-ray quickly because the beam is very small (only 0.05 mm vertically, which is the direction the shutter moved into the beam). From the current in an ionization chamber, it was judged that the shutter closed in 0.6 ms (Fig. 3*a*). Images of the beam were recorded using an X-ray image intensifier coupled with C7770. The number of pixels in the vertical direction was 18, so that the time resolution was 0.164 ms.

Fig. 3(*a*) shows the intensity recorded, after closing the shutter, by an X-ray image intensifier with P46. There may be a delay of 0.1–0.2 ms, but it is a very weak persistence. It should be noted that this

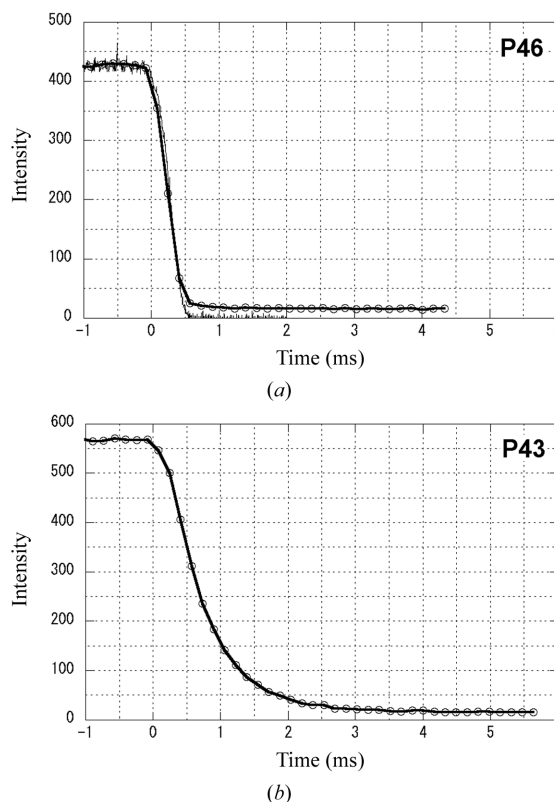


Figure 3 Persistence of two phosphors that are used in X-ray image intensifiers. (a) P46, (b) P43. In (a), the current in an ion chamber (S-1329A, Oken, Tokyo, Japan) is also shown. The X-ray shutter began to cut the beam at time zero. The final level of the decay corresponds to the offset of the analogue-to-digital converter.

persistence may not be that of P46 but could be that of CsI which is used in the front window of the image intensifier. On the other hand, when P43 was used, the persistence was much more prolonged (Fig. 3*b*).

3.2.3. Data example: skeletal muscle diffraction. A diffraction pattern from a frog muscle (sartorius muscle from a bullfrog, *Rana catesbeiana*) was recorded at BL40XU without attenuation. With 640×72 pixels in an image, only the meridional region was recorded, with a time resolution of 0.53 ms (Fig. 4*a*). Since the muscle was set vertically, the camera was rotated by 90° so that the meridian of the diffraction pattern was parallel to the longer side of the image. The integrated intensity of the third-order meridional reflection from the thick filament, at $1/145 \text{ \AA}^{-1}$, was measured. To avoid radiation damage, the muscle was moved vertically at a speed of 100 mm s^{-1} during the experiment (Yagi, 2003). When the muscle was tetanically stimulated by electrical pulses at 278 K and its length was reduced by about 1% instantaneously, a sudden transient decrease in intensity, similar to that observed in previous studies using a gas detector

(Irving *et al.*, 1992; Bordas *et al.*, 1995), was observed (Fig. 4*b*). One notable difference from the previous study was that the data set in Fig. 4*b* was obtained in a single contraction experiment, while those in previous studies were obtained by addition of data from hundreds of runs.

With C7770 it is necessary to reduce the size of an image to achieve a high time resolution. This is sometimes found to be inconvenient. One way of overcoming this problem is to use a rotating shutter that is synchronized with the frames of the CCDs. An apparatus for this technique has been developed. Frame signals from the CCDs are used to rotate a tantalum disk at $145.5 \text{ rotations s}^{-1}$. This disc has a pair of arcs on opposite sides across the centre. The arc crosses the X-ray beam 291 times per second, that is once in a CCD frame. The disc has several pairs of arcs of different lengths so that an exposure time in each frame can be chosen (Fig. 4*c*). The interval between the frame signal and the X-ray exposure ('delay' in Fig. 4*c*) can be changed by a delay generator (DG-535, Stanford Research Systems, Sunnyvale, CA, USA). By repeating an experiment with different delays it is possible to divide a 3.4 ms frame into many subframes. Then, by arranging the subframes after the experiment, continuous time-resolved images are obtained. This technique requires that the experiment can be repeated several times under the same conditions. When this is realised, the time resolution is not limited by the frame rate of the CCD.

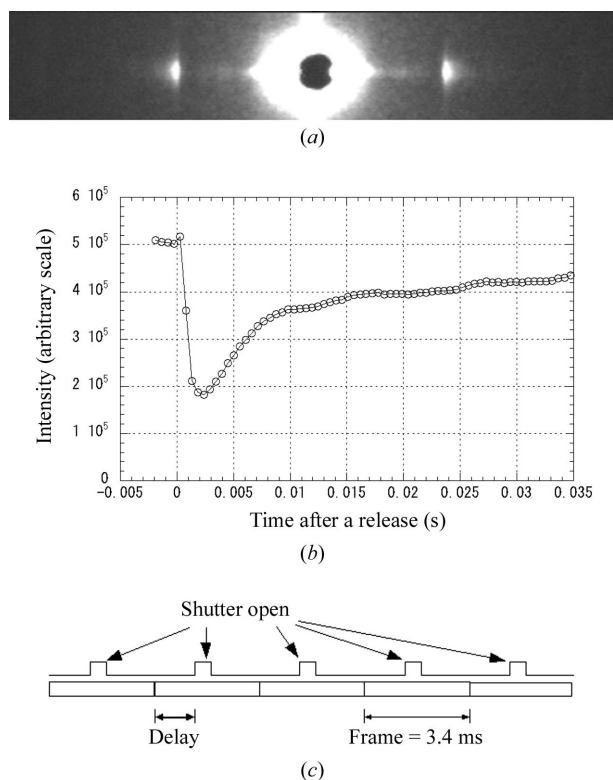


Figure 4
An X-ray diffraction study on skeletal muscle contraction. (a) A meridional region of the diffraction pattern from an isometrically contracting frog muscle. In the centre, a backstop and a scatter are observed. The two strong peaks on both sides are the third-order meridional reflections from the myosin filaments (at $1/145 \text{ \AA}^{-1}$). The exposure time was 0.53 ms. The image size was 640×72 pixels. The temperature was 278 K. (b) The intensity change of the myosin meridional reflection (14.5 nm) after a quick release of the muscle with an amplitude of about 1%, which completes in 1 ms. The data set was obtained in a single run. The fluctuation seen during the intensity recovery is probably due to changes in the muscle thickness: since the muscle was moved continuously to avoid radiation damage during the experiment, the part of the muscle that was irradiated changed continuously and the muscle thickness may vary with time (Yagi, 2003). (c) Timing diagram to show how a time resolution higher than the frame rate can be achieved by using a rotating shutter. As the shutter is synchronized with the frames, it is possible to pass the X-rays at the same timing in all frames. By changing the delay time and combining all data afterwards, it is possible to obtain continuous time-resolved data with an exposure time shorter than the frame length.

3.3. C7770 with a high-resolution detector

3.3.1. Persistence. Persistence measurements were made as described in §3.2.2. Fig. 5(a) shows a persistence curve of P43 used in the high-resolution detector (BM2). As was found with the X-ray image intensifier (Fig. 3*b*), the persistence lasts for about 3 ms. The difference from the data in Fig. 3(i) is that the phosphor is directly excited by X-rays, not by electrons.

In order to increase the time resolution, other types of phosphors have also been tested. P46 (YAG:Ce), which is used in the X-ray image intensifier, can also be used (Koch *et al.*, 1998; Terasaki *et al.*, 2004). However, since most imaging experiments at SPring-8 are carried out with high X-ray energies, a scintillator with higher stopping power is preferred. Fig. 5(b) shows a persistence curve of a single crystal of LSO ($\text{Lu}_2\text{SiO}_5:\text{Ce}$). Although there seems to be a very low level of long-lasting luminescence over several milliseconds, the persistence is not distinct. This scintillator has a high density, and thus it may be useful in experiments with high time resolution using high-energy X-rays.

3.3.2. Data example: coronary angiography. Coronary angiography requires high spatial resolution to visualize fine coronary arteries and veins. In order to observe the coronary blood flow during a heartbeat using a contrast agent, a seamless recording with high time resolution is necessary. High time resolution is also required because the heart moves when it beats. High spatial resolution requires even higher time resolution because a very small movement of the heart will blur the image. Thus, this is a technically challenging experiment. An experiment was carried out at BL20XU, which provides a flux that is high enough for the required time resolution. Fig. 6 shows a radiogram of a rat heart recorded in 3.4 ms using a high-resolution detector (BM2 with P43) and C7770. A contrast agent was infused through the coronary artery from the aorta. Although the rapid movement of the X-ray beam due to vibration in the monochromator (this was also improved later) made it difficult to observe a fixed part of the heart continuously, blood vessels with diameters down to $\sim 20 \mu\text{m}$ are visualized (Fig. 6).

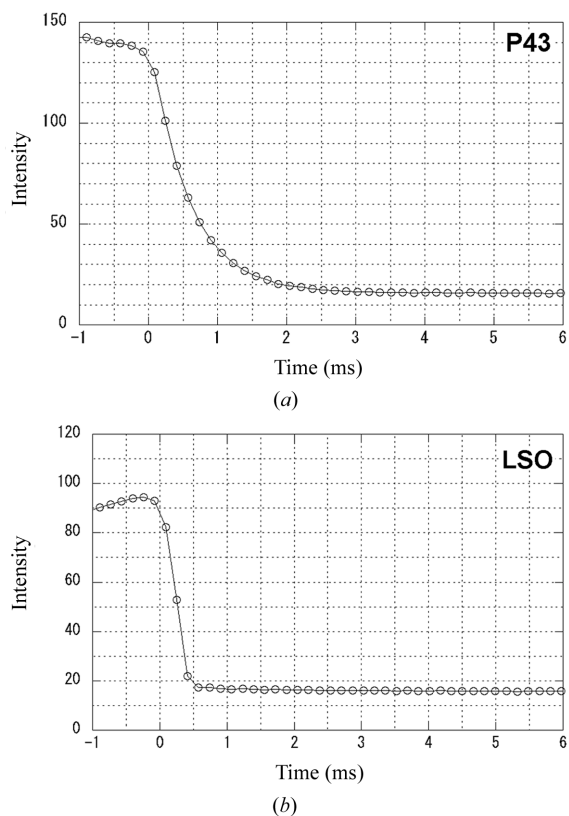


Figure 5 The persistence of two phosphors that are used in high-resolution imaging detectors. (a) P43, (b) LSO. The X-ray shutter began to cut the beam at time zero. The intensity change seen before time zero is probably due to the beam intensity fluctuation caused by vibration of the focusing mirrors.

The total beam flux at 17 keV was about 1×10^{12} counts s^{-1} when this experiment was performed (it was improved by more than one order of magnitude later). From the total counts in a beam without a specimen, it is estimated that about 200 X-ray photons are required to create 1 ADU in the CCD camera, that is 0.1 electrons per X-ray photon. This low conversion gain is due to (i) the use of a thin phosphor (10 μm), which is necessary for high-resolution imaging, (ii) the low efficiency of the lens coupling (Liu *et al.*, 1994), and (iii) the low sensitivity of the CCD camera, which is described in §3.2.1.

4. Discussion and concluding remarks

In the third-generation synchrotron radiation facilities, many time-resolved experiments that require area detectors are being carried out. In addition to the experiments described here, time-resolved protein solution scattering experiments (for example, Akiyama *et al.*, 2002), time-resolved XAFS experiments (Allinson, 1989), time-resolved radiography experiment for viscosity measurements (for example, Terasaki *et al.*, 2004) and very fast tomographic imaging experiments (Lame *et al.*, 2003) all require an area detector with high time resolution in the microsecond to millisecond range. For these experiments the CCD camera described here may be useful. Since the use of a prism makes it impossible to directly illuminate CCD chips with X-rays, conversion of X-rays into visible light using a phosphor scintillator is essential. The two types of X-ray detectors described here, an image intensifier and a phosphor–lens system, combine well with the camera. The use of a precision mount between an X-ray detector and a camera makes both versatile. A camera can be

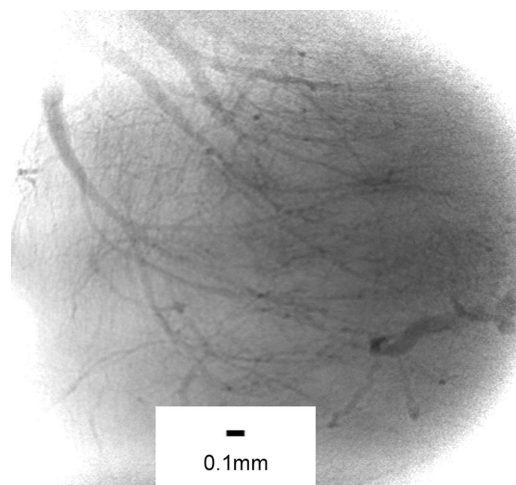


Figure 6 Image of coronary blood vessels in a rat heart. Only a small (about 3 mm \times 3 mm) region is shown. A contrast agent (iopamiron) was injected into the coronary artery from the aorta. The exposure time was 3.4 ms. The pixel size was 7 μm \times 7 μm .

combined with different X-ray detectors for various purposes, and *vice versa*. This increases the number of applications in which the detector can be used. Good examples of such versatility are the muscle diffraction and angiography experiments presented here. We have also used the combination with the high-resolution detector for beam diagnosis in a top-up operation: a shift of an X-ray beam after an injection of electrons into the storage ring was studied at a time resolution of 0.16 ms. In this case, the persistence of P43 considerably affected the time resolution of the recorded images.

Although the high frame rate is an attractive feature, care must be taken when using this camera. Its unique 3-CCD design means that some data corrections are necessary. However, these are not difficult when the calibration data are recorded during the experiment. One disadvantage of a fast camera in general is the narrow dynamic range. The dynamic range of this camera, as defined by the ratio of the well depth and the readout noise, is about 1500. The 10-bit AD converter is sufficient to cover this range. Considering that most high-speed cameras have an 8-bit ADC, this dynamic range is useful for quantitative purposes. Also, the camera is less sensitive than slow-scan cooled CCD cameras. The combination of the X-ray image intensifier and C7770 is not sensitive enough to detect a single photon. This is partly due to the use of P46, which emits only about one-third of light compared with other phosphors such as P20 or P43 (T. Endo, personal communication). Thus, this detector should be used at a beamline where the X-ray intensity is sufficiently high. On the other hand, when the image can be recorded, the photon statistics are not a serious problem because the number of photons is already quite large, as shown in Fig. 4.

Although C7770 is a fast camera, its performance as an X-ray detector is limited to some extent by the persistence of the phosphor scintillator. The choice of the X-ray detector that is used with the camera is important. The X-ray image intensifier with P46 phosphor is an ideal detector for small-angle diffraction and scattering experiments. Hamamatsu Photonics have discontinued the production of the six-inch image intensifier described here. However, a four-inch image intensifier with a beryllium window, which has better spatial resolution than that of the six-inch, is still available. Combination with a high-resolution imaging detector has also been found to be useful, but a phosphor with a persistence shorter than the time resolution of the detector should be used.

There may not be many cases where the combination of an X-ray image intensifier and a fast CCD camera is the only way to cope with the high flux: the highest count rate (1.5×10^7 counts s^{-1} in global count rate) achieved by a gas detector (Lewis *et al.*, 2000) is usually sufficient. However, the detector system presented here has the advantage that it is less expensive (<200 000 USD) and commercially available. Since there are no mechanical parts in the detector and neither a gas nor a liquid is used, the reliability of the detector system is quite high: it has been used on beamline BL40XU at SPring-8 without major trouble for three years and has proved to be an important tool in time-resolved diffraction experiments, especially in the field of muscle physiology (Yagi, 2003; Wakayama *et al.*, 2004).

In conclusion, it has been shown that a submillisecond time-resolved experiment can be performed using a fast CCD camera. The choice of the phosphor that converts X-rays to visible light is important in the design. Its capability has been demonstrated in diffraction and imaging experiments.

We thank Drs Y. Ogasawara, T. Matsumoto and H. Tachibana (Kawasaki Medical School) and Drs Y. Suzuki and K. Umetani (SPring-8/JASRI) for their help in the angiography experiment at BL20XU, Dr H. Iwamoto (SPring-8/JASRI) for the skeletal muscle experiment at BL40XU, Drs K. Uesugi and T. Sera (SPring-8/JASRI) for the persistence measurements of the high-resolution detector, and Mr T. Maruno and T. Endo (Hamamatsu Photonics KK) for construction of the prototype detector. Experiments were carried out with the approval of the Program Review Committee of SPring-8 (2000A0450-NL-np, 2000A0454-NL-np, 2002A0057-NL2-np, J01B20XU-0502-N, 2002A0174-NL2-np). This work was supported by the SPring-8 Joint Research Promotion Scheme of the Japan Science and Technology Corporation and Active Nano-Characterization and Technology Project (Special Coordination Funds of the Ministry of Education, Culture, Sports, Science and Technology of the Japanese Government).

References

- Akiyama, S., Takahashi, S., Kimura, T., Ishimori, K., Morishima, I., Nishikawa, Y. & Fujisawa, T. (2002). *Proc. Natl. Acad. Sci. USA*, **99**, 1329–1334.
- Allinson, N. M. (1989). *Nucl. Instrum. Methods*, **A275**, 587–596.
- Amemiya, Y., Ito, K., Yagi, N., Asano, Y., Wakabayashi, K., Ueki, T. & Endo, T. (1995). *Rev. Sci. Instrum.* **66**, 2290–2294.
- Bordas, J., Lowy, J., Svensson, A., Harries, J. E., Diakun, G. P., Gandy, J., Miles, C., Mant, G. R. & Towns-Andrews, E. (1995). *Biophys. J.* **68**, 99s–105s.
- Fujisawa, T., Inoko, Y. & Yagi, N. (1999). *J. Synchrotron Rad.* **6**, 1106–1114.
- Gruner, S. M. & Ealick, S. E. (1995). *Structure*, **3**, 13–15.
- Horiuti, K., Yagi, N., Takemori, S. & Yamaguchi, M. (2003). *J. Biochem.* **133**, 207–210.
- Hülsen, G., Eikenberry, E. F., Horisberger, R., Schmitt, B., Schulze-Briese, C., Tomizaki, T., Toyokawa, H., Stampanoni, M., Borchert, G. L., Willmott, P., Patterson, B. & Brönnimann, Ch. (2004). *AIP Conf. Proc.* **705**, 1009–1012.
- Inoue, K., Oka, T., Miura, K. & Yagi, N. (2004). *AIP Conf. Proc.* **705**, 336–339.
- Inoue, K., Oka, T., Suzuki, T., Yagi, N., Takeshita, K., Goto, S. & Ishikawa, T. (2001). *Nucl. Instrum. Methods*, **A467/468**, 674–677.
- Irving, M., Lombardi, V., Piazzessi, G. & Ferenczi, M. A. (1992). *Nature (London)*, **357**, 156–157.
- Koch, A., Raven, C., Spanne, P. & Snigirev, A. (1998). *J. Opt. Soc. Am.* **A15**, 1940–1951.
- Lame, O., Bellet, D., Di Michiel, M. & Bouvard, D. (2003). *Nucl. Instrum. Methods*, **B200**, 287–294.
- Lewis, R. A., Berry, A., Hall, C. J., Helsby, W. I. & Parker, B. T. (2000). *Nucl. Instrum. Methods*, **A454**, 165–172.
- Liu, H., Karellas, A., Harris, L. J. & D'Orsi, C. J. (1994). *Med. Phys.* **21**, 1193–1195.
- Rossi, G., Renzi, M., Eikenberry, E. F., Tate, M. W., Bilderback, D., Fontes, E., Wixted, R., Barna, S. & Gruner, S. M. (1999). *J. Synchrotron Rad.* **6**, 1096–1105.
- Suzuki, Y., Uesugi, K., Takimoto, N., Fukui, T., Aoyama, K., Takeuchi, A., Takano, H., Yagi, N., Mochizuki, T., Goto, S., Takeshita, K., Takahashi, S., Ohashi, H., Furukawa, Y., Ohata, T., Matsushita, T., Ishizawa, Y., Yamazaki, H., Yabashi, M., Tanaka, T., Kitamura, H. & Ishikawa, T. (2004). *AIP Conf. Proc.* **705**, 344–347.
- Terasaki, H., Kato, T., Funakoshi, K., Suzuki, A. & Urakawa, S. (2004). *J. Phys. Condens. Matter*, **16**, 1707–1714.
- Uesugi, K., Tsuchiyama, A., Nakano, T., Suzuki, Y., Yagi, N., Umetani, K. & Kohmura, Y. (1999). *Proc. SPIE*, **3772**, 214–221.
- Wakayama, H., Tamura, T., Yagi, N. & Iwamoto, H. (2004). *Biophys. J.* **87**, 430–441.
- Yagi, N. (2003). *Biophys. J.* **84**, 1093–1102.